Volume plasmon ejection of ions in pulsed ultraviolet laser induced desorption from several metals

David P. Taylor* and Henry Helvajian
Physical Sciences Laboratory, The Aerospace Corporation, 2350 El Segundo Boulevard, El Segundo, California 90245, USA
(Received 9 January 2008; revised manuscript received 23 December 2008; published 5 February 2009)

A study of pulsed UV laser induced desorption (LID) at 248 nm has been performed on several single-crystal metal samples: Al(111), W(100), and Ni(111). It has been found that for each sample the kinetic-energy distribution of the desorbed ions is sharply peaked at the volume plasmon energy. The acceleration of an ion through interaction with an electromagnetic wave at the surface of a conductor provides unambiguous evidence that volume plasmons are excited in the metal samples during these LID experiments. Our data indicate that the pulsed UV laser photons can excite volume plasmons in the metal sample with quantum energies three or more times the energy of a single photon. This experimental observation provides strong support for the notion that volume plasmons can play an important role in laser-surface interactions, and a few of the implications of this notion are discussed.

DOI: 10.1103/PhysRevB.79.075411 PACS number(s): 73.20.Mf, 71.45.Gm, 71.45.Lr

I. INTRODUCTION

The behavior of light impinging on a polished metal surface is often used as a textbook example of the interaction of electromagnetic waves and metals. While the system is familiar to anyone who has looked into a mirror, it has aspects that still might be able to challenge some of our preconceptions. The problems begin with the physical discontinuity at the surface. Other difficulties arise as the intensity of the light increases above a low level and as the photon energy approaches the plasmon energy.[1,2] It is possible to access both of these regimes with experimental techniques involving the interaction of particle and electromagnetic fields in the near-surface region, such as UV photoemission and photon-stimulated desorption (PSD).

Experiments involving photon-stimulated desorption of ions have a long history. In the low-intensity regime, characterized by a linear dependence of desorption yield on intensity, absorption of a sufficiently energetic photon is required to activate the desorption process. Depending on the photon energy and the experimental system, ion desorption can proceed through processes ranging from Knotek-Fiebelman[3] to Menzel-Gomer-Redhead (MGR) (Refs. 4 and 5) mechanisms. In the Knotek-Fiebelman case, absorption of a sufficiently energetic photon can lead to an interatomic Auger process and can result in ion desorption through local inversion of the Madelung potential. In the MGR process, desorption takes place when photoabsorption promotes an adatom-surface-bound electronic state to an antibonding state.

Laser experiments have allowed access to the high-intensity regime. This is often characterized by high-order photon absorption sometimes due to absorption in the plume, and a daunting number of processes then become possible.[6] There can be extreme thermal spikes and shock waves in and around the laser spot. An excess of high-kinetic-energy (KE) ions in the tails of thermal distributions can often be observed, and this has been attributed to photoabsorption in the plume of laser induced desorption (LID) experiments. The well-established physical picture for this high laser fluence regime involves a threshold or thermal process. There is ample support that this threshold or thermally mediated picture is valid, particularly in the high laser fluence regime (see, for example, Ref. 2). A standard way of approaching this problem has been to extend the Fowler-Dubridge photoemission model to higher-order processes.[7] While this desorption behavior is the expected process, it is not the only sort of laser material interaction process that can take place. Even minority laser material interaction processes can exhibit interesting and useful behavior, e.g., x-ray harmonic generation.[8]

At lower intensities, laser experiments offer access to other physical processes. These include the surface-enhanced Raman effect[9,10] and multiphoton photoemission.[11,12] Other phenomena that occur in this intensity regime include the plasmon photoexcitation in clusters and nanoparticles (see, for example, Refs. 13–17). The excitation of plasmons in free clusters and nanoparticles on or inside substrates presents a way to resonantly access these particles. It is possible to control the size and shape of the particles. Laser excitation of surface plasmons in thin films using the attenuated total reflection (ATR) geometry can lead to desorption through both single-photon and multiphoton processes.[18,19]

Plasmon excitation is known to play a role in a variety of experiments involving charged particle–surface interactions. This behavior is perhaps most familiar in charged particle penetration experiments.[20] Surface and volume plasmon interactions with charged particles moving near a surface are also possible. One example is the acceleration of charged particles moving near a grating or real-world surface by the Smith-Purcell effect.[21–25] Theoretical support for experiments involving the excitation of volume plasmons by charged particles moving near a metal surface was provided by Beraga *et al.*[26]

Laser experiments often seem to access somewhat different results from the traditional light sources in photon-stimulated desorption experiments. LID experiments often produce ions with a Maxwell-Boltzmann kinetic-energy distribution associated with laser ablation related surface melting and photoionization in the ablation plume.[27] Occasionally, laser induced desorption experiments have been

observed to deviate from this expected thermal result.[11,28–32] There are experiments which clearly point to surface plasmon involvement in laser stimulated desorption experiments.[33] The set of experiments reported here is intended to elucidate the somewhat contradictory results of a group of relatively low fluence nanosecond pulsed UV LID experiments that appear to involve volume plasmon excitation.

Helvajian and Welle[34] performed a LID experiment involving the pulsed UV laser illumination of the front side of a Ag(111) crystal surface that resulted in a silver-ion kinetic-energy distribution rather sharply peaked at 9 eV. Shea and Compton[35] performed an experiment on a silver surface and found a thermal distribution peak with a second kinetic-energy peak at about 3.5 eV. The 9 eV result of Helvajian and Welle[34] corresponds to the volume plasmon energy of silver, and the 3.5 eV result of Shea and Compton[35] corresponds to the surface plasmon energy of silver.

Kim and Helvajian[36] reported pulsed UV LID ion kinetic energy results for Al(111) that are inconsistent with either the volume plasmon or the surface plasmon energy of aluminum. The vacuum conditions, surface preparation, laser control, electronics, and general setup of the experiment were improved; this Al(111) LID experiment was repeated at several laser wavelengths; and the Taylor and Helvajian[37] result was that 15 eV kinetic-energy aluminum ions were observed in each case. The Al(111) pulsed UV LID result was that the desorbed ions left with a kinetic-energy distribution that was sharply peaked at the volume plasmon resonance energy for aluminum.

Ritchie *et al.*[38] explained the experiment of Shea and Compton[35] as a surface plasmon annihilation at a metal surface resulting in a transfer of momentum to an ion in the near-surface region. Because of this support, the Ag(111) surface plasmon result of Shea and Compton[35] is perhaps the most consistent with expectations. However, Ritchie *et al.*[38] considered including a volume plasmon annihilation momentum-transfer mechanism in that paper and found no compelling reason that would preclude such a process from occurring.[39]

The work reported here extends the LID experimental results for aluminum to tungsten and nickel and improves the aluminum experiment. In each case the pulsed UV LID ion kinetic-energy distribution was found to be sharply peaked on the samples' volume plasmon energy.

II. EXPERIMENT

Our experimental setup employed a modified Wiley-McLaren 1.7 m time-of-flight (TOF) mass spectrometer with multichannel plates to detect ions desorbed in a small solid angle about the surface normal. A small 248 nm excimer pulsed laser beam with an angle of incidence of about 45° impinges on a polished metal single crystal in an ion-pumped UHV chamber. The experiments were usually performed with a background pressure of about 3×10^{-10} Torr, but some of the work was performed at pressures as high as 2×10^{-9} Torr. The 248 nm laser was loosely focused to an area of about 0.1 mm^2 on the sample, and the laser fluence was approximately 10 MW/cm^2 or 100 mJ/cm^2 in a 10 ns pulse. Data were collected with a Computer Automated Measurement and Control (CAMAC)-based 100 MHz transient digitizer connected to the amplified multichannel plate output.

The LID experiments reported here have been conducted using laser pulses with a photon energy well below the volume plasmon frequency of the metal sample. In these LID experiments, not every laser shot produces target ion signal at our multichannel plate detector which is located more than 1.5 m from the sample.

The attempt is made to operate under conditions wherein we detect single ions of the same material as the sample when a laser shot does produce signal. The laser intensities in the LID experiments are above the intensity of light sources typical of many PSD experiments and may be closer to the laser fluences used in surface-enhanced Raman spectroscopy. This regime is below the intensity threshold at which surface melting is observed and the surface of our samples appears visually unchanged after many thousands of laser shots. For longer exposures, some cumulative changes in the surface morphology are observed (see Ref. 40), and more of these data will be reported separately. There is a brief initial period (over tens of laser shots) during which the ion product yield can change significantly, and we associate this with cleaning the surface. Changes in the surface roughness of the samples over longer times may lead to some changes in the ion yield but do not appear to alter the kinetic-energy distribution of the ions. It is possible that our TOF experimental setup—with a roughly 45° laser incidence, perpendicular TOF geometry, and small solid angle of collection at low-voltage differences in the extraction region—plays a significant part in selecting the ions that we observe.

This work was performed using laser-pulse intensities close to the threshold for detection of ions. The signal-to-noise ratio in this work was enhanced by summing the mass spectra from many laser shots while using software discrimination to suppress the background. The extraction voltage was varied incrementally and the measured ion arrival time was compared with calculated arrival times for different initial ion kinetic energies systematically over the entire range of extraction voltages. Both of these experimental approaches were developed and used in earlier time-of-flight photoelectron kinetic-energy analysis experiments.[41–44] Refer to Ref. 37 for additional details and specific results from pulsed UV LID experiments performed on Al(111) with 266 and 355 nm light.

The aluminum LID experiment usually featured Al^+ as the major peak in the mass spectra (see Fig. 1). Typical impurity ion peaks in the aluminum mass spectrum were consistent with potassium, sodium, and aluminum oxide. LID of W^+ ions from W(100) gave a recognizable isotope pattern but a much smaller signal than that of Al^+ from Al(111).

Tungsten (i.e., W^+) was usually the dominant peak in the W(100) experiment (refer to Fig. 2). Typical tungsten impurity TOF mass peaks were consistent with K^+, Na^+, and WO^{++} ions. We also note that the laser fluence had a significant impact on our ability to resolve different isotope peaks in the TOF mass spectra. This can be seen in the comparison of the tungsten isotope peak resolution collected under similar experimental conditions except for laser power shown in

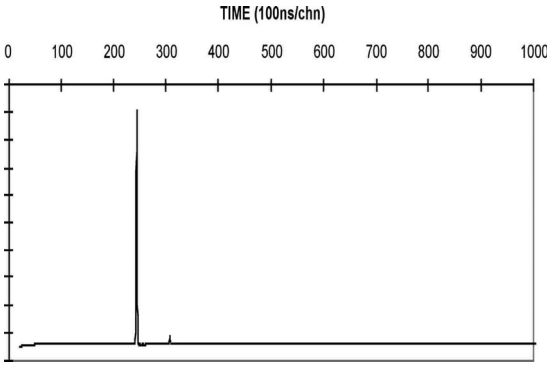

FIG. 1. Time-of-flight mass spectrum for the 248 nm pulsed laser induced desorption of aluminum from an Al(111) crystal. The spectrum shows the impurity profile. Impurity peaks that are most often observed are consistent with potassium, sodium, and aluminum oxide ions (which is visible as a small peak in this mass spectrum). Typically, these impurity peaks are most easily observed after the sample has been in the vacuum chamber some hours after sample preparation (e.g., surface preparation using argon-ion sputtering).

Fig. 3. Impurity ion peaks dominated the LID mass spectra in the nickel experiment. LID of Ni^+ ions from Ni(111) produced a quite small signal surrounded by much larger impurity peaks.

Figure 3 shows (20 ns/channel) mass spectra of ion peaks assigned to tungsten from a 248 nm LID experiment on a W(100) crystal. These data were collected with a low-voltage extraction bias between the sample and the first plate in the TOF mass spectrometer. The experimentally observed isotopic resolution is possible only if the ions leave the surface promptly with a narrow kinetic-energy distribution and an initial ion kinetic energy of at least several electron volts: if the ion kinetic energy was approximately thermal there would be broad peaks without isotope separation in the tungsten mass spectra at low Wiley-MacLaren extraction voltages.

III. RESULTS

Figures 4 and 5 present 248 nm 10 ns/channel pulsed LID TOF arrival time data and calculated arrival times for tungsten. A section of the data from Fig. 4 is presented again in a more detailed view in Fig. 5.

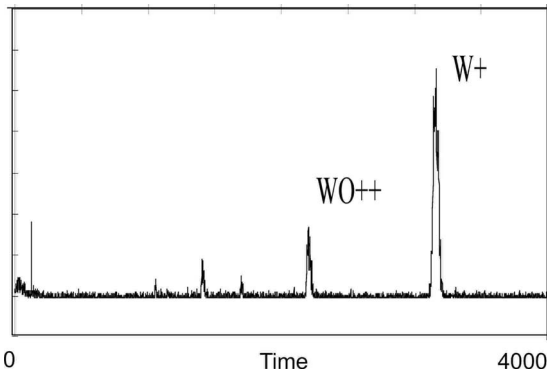

FIG. 2. TOF mass spectrum for the 248 nm pulsed LID of tungsten ions from a W(100) crystal. The TOF data from a 20 ns per channel transient digitizer were summed. The major TOF ion peak is attributed to tungsten. The largest impurity peak observed is consistent with doubly charged tungsten oxide ions.

The calculated arrival times were determined using measured distances and voltages for the time-of-flight system. The only remaining parameter in the arrival time model is small constant shift in start time that is associated with the instrument electronic response, the experimental geometry, and our triggering scheme. This instrument response time is small and fixed for each experiment, and varies only slightly over the entire course of work reported in this paper. We have used this method for other TOF kinetic-energy analysis and have developed confidence in it over the years.[41] One of the main sources of error was a small uncertainty in the distance between the sample and the first plate in the time-of-flight mass spectrometer, which could be eliminated in a different experimental setup. Except for the nickel experiment, the ion TOF kinetic-energy measurement at these energies is easier than the previous photoelectron TOF kinetic-energy measurements. The experimental instrument response time correction allows the calculated and experimental ion arrival times to agree in the asymptotic limit at high extraction voltages for the entire range of observed ion masses (under conditions where the initial ion kinetic energy has a negligible contribution on the ion arrival time).

In this group of experiments, we vary the extraction voltages. The ion arrival times in the high extraction voltage range confirm the identity of the ion peak and the constancy of the calculated and experimental arrival times. Incremental changes in the extraction voltage make it clear that we are looking at the same ion peak at lower extraction voltages, where the initial ion kinetic energy has the largest contribution to the arrival times. The kinetic-energy analysis of our data involves the comparison of the shape of the ion arrival time versus extraction voltage curves for the experimental data and calculations for ions with different initial kinetic energies. The calculated and experimental arrival times agree over the entire range of extraction voltages when the appropriate initial ion KE is included in the arrival time calculation (see Fig. 4.).

At low extraction voltages, the ion initial KE has a significant contribution to the ion arrival time. The low extraction voltage range of the data in Fig. 4 appears in Fig. 5. The kinetic energy of the tungsten ions was found to be 22 ± 3 eV. At lower extraction voltages, the isotope peaks become broader and more asymmetric, and overlap more: this loss of resolution for isotope peaks in the TOF mass spectrum accounts for the scatter in the data of Fig. 5 and throughout this set of experiments. The experimental and calculated arrival times of nickel-ion peaks from a 248 nm LID experiment on Ni(111) are compared as before in Fig. 6 and in more detail in Fig. 7.

The pulsed UV LID signal for nickel ions is the smallest of the metals examined so far. The low nickel-ion signal and the high kinetic energy of the observed ions complicate this experiment more than the others. The loss of isotope peak resolution can explain the deviation of the experimental points from the uppermost arrival time curve in Fig. 6. The kinetic energy of the nickel ions was determined to be 30 ± 5 eV. Additional support for the volume plasmon picture is provided by the contaminant potassium 39 amu iso-

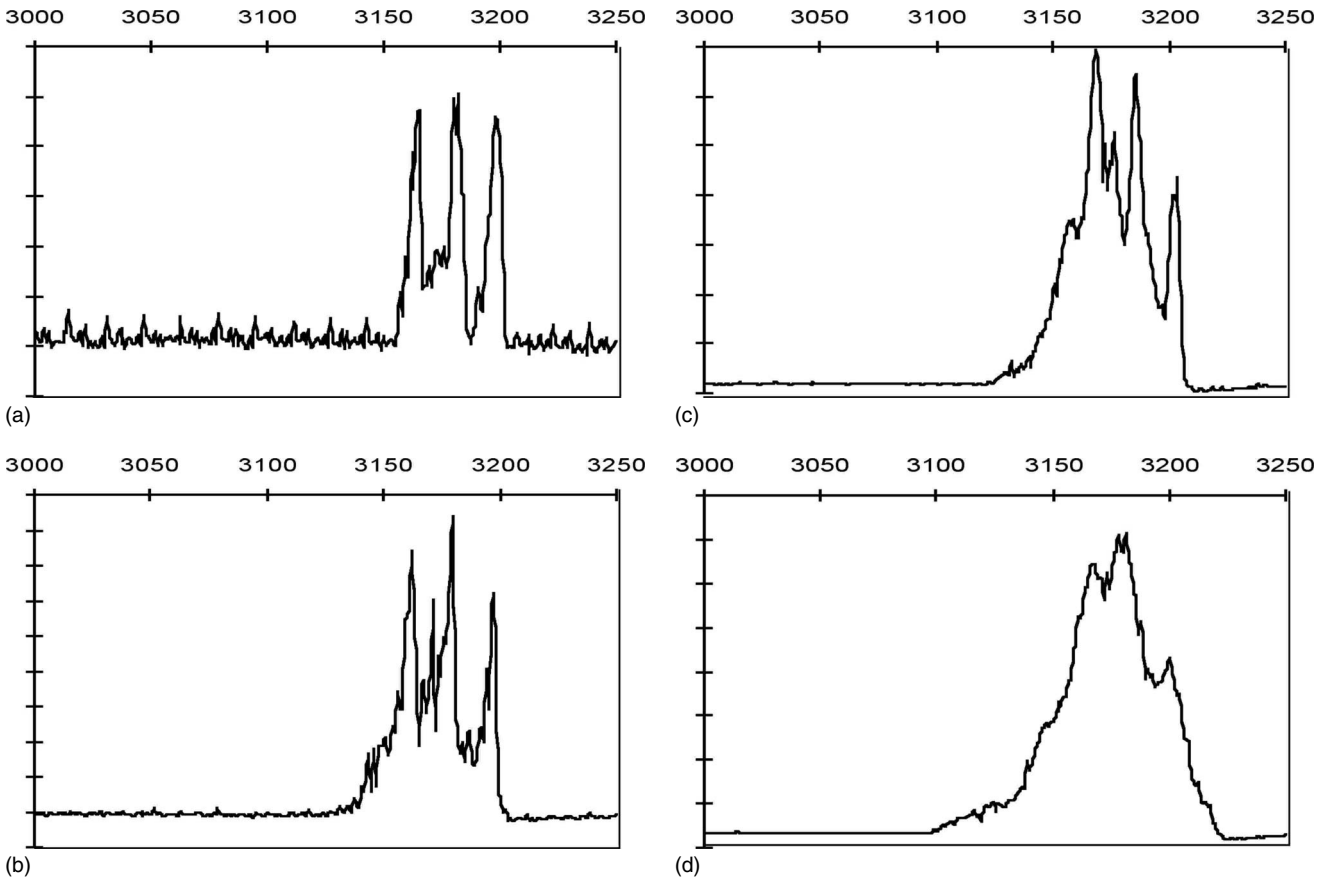

FIG. 3. Tungsten W^+ isotope peaks in LID TOF mass spectrum. The extraction voltage was +200 V, and the total voltage was +900 V. The ion arrival times were collected using a 20 ns per channel digitizer. The 248 nm laser was loosely focused, and the intensities were measured in collecting these data. Tungsten isotopes' abundances: minor isotope 180 amu, 0.14%; 182 amu, 26.4%; minor isotope 183 amu, 14.4%; 184 amu, 30.6%; and 186 amu, 28.4%. [(a) 280 μJ; (b) 290 μJ; (c) 310 μJ; and (d) 340 μJ.]

tope peak from Ni(111), which also exhibits about 30 eV of kinetic energy and is included in both Figs. 6 and 7. In both the tungsten and nickel mass spectra, the proximity and overlap of the isotope peaks may account for the slight shift in the measured apex of those ion arrival time peaks from the calculated arrival time curves.

A similar kinetic-energy analysis of the arrival time data of Al^+ from Al(111) is presented in Figs. 8–10. In Fig. 10, several initial kinetic energies are used to calculate the ion arrival times: these calculated arrival times are subtracted from the experimental arrival times for several extraction voltages. In this treatment of the data, a horizontal line indicates a good fit and a constant shift in the experimental arrival time would only move the arrival time difference curve up or down. This approach to data analysis confirms that the ion initial kinetic-energy determination is not changed much by a contribution from the instrument response time correction. The Al^+-ion kinetic energy is found to be 15 ± 2 eV, the volume plasmon energy of aluminum.

Although we work in a regime where many laser shots do not produce target ions, some laser shots produce bursts of multiple ions. The space-charge interaction between ions in the TOF spectrometer has the effect of broadening the ion TOF arrival time peaks (see Fig. 11). As part of the Al(111) LID experiment, we stored a time slice of the TOF mass spectra for every laser shot along with the laser power. The laser power did not seem to correlate with the periods where bursts of ions were more frequently observed. Some attempts were made to investigate laser polarization in these experiments without success. This ion yield bursting behavior seemed to dominate any change in ion yield that might have been associated with laser polarization in this set of experiments. While there are some ways that the polarization might still have been studied, they could not be implemented in the time available. To correct for space-charge effects for Al^+ ions within the TOF tube we summed only the mass spectra with single-Al^+-ion hits (see Fig. 12). This approach narrows the earlier Al^+ peak kinetic-energy estimate of Ref. 37 to a full width at half maximum of about 2 eV for 248 nm LID of Al(111) (see Fig. 13).

In each of the metals studied by pulsed UV LID, the ion kinetic-energy peaks are relatively sharply centered on the volume plasmon energy of the sample. The impurity peaks we have studied also have kinetic-energy distributions that are sharply peaked at the volume plasmon energy of the sample. While many impurity peaks are observed, the kinetic-energy distributions of all the ion peaks are remarkably free from background contributions, including some that we might expect to observe. We do not observe the thermal ion distributions that we have seen in laser ablation

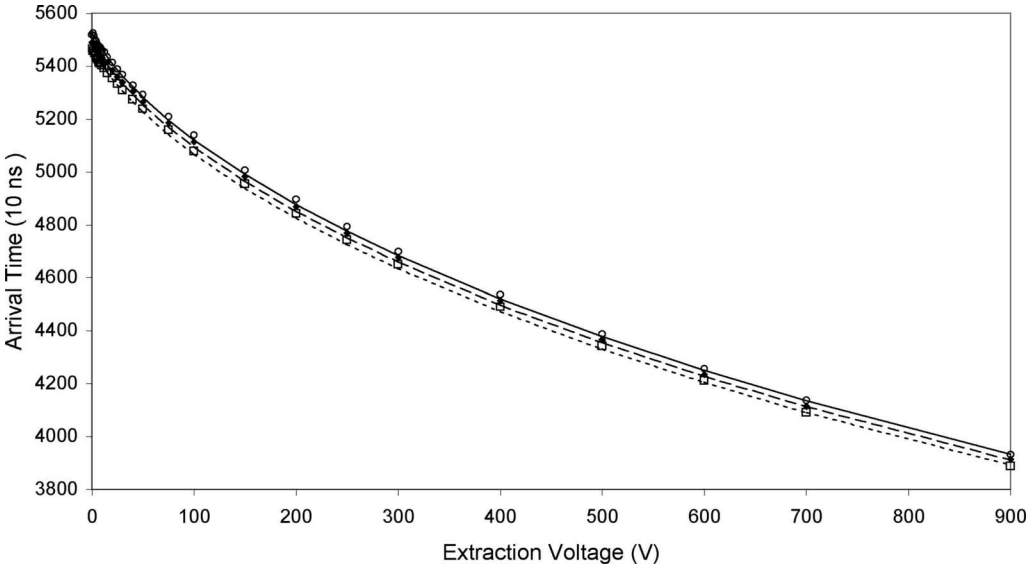

FIG. 4. Kinetic-energy determination of LID of W(100) at 248 nm and 10 ns per channel taken with software discrimination. The sample was held at +1400 V plus the indicated extraction voltage and the voltage bias of the first plate of the mass spectrometer was measured to be +1400 V. Experimental arrival times for peaks assigned to tungsten isotopes: 182 amu (squares); 184 amu (triangles); and 186 amu (circles). Minor isotopes 180 and 183 amu are not indicated. The calculated ion arrival times with 22 eV initial kinetic energy are indicated as lines in the figure: 180 amu (solid line), 182 amu (dashed line), and 184 amu (dotted line).

experiments. We also do not see evidence of surface plasmon peaks or multimode plasmon kinetic-energy peaks in our TOF data. It may be that our experimental geometry plays a role in this observation since our setup collects a relatively small solid angle around the surface normal for low extraction voltages.[45] Table I compares our measured results with both theoretically predicted and experimental volume plasmon energies listed in the book by Pines.[46]

IV. DISCUSSION

The usual experience in laser stimulated desorption experiments is to end up with a nearly thermal product kinetic-energy distribution that can be reconciled to the melting temperature of the sample, possibly by assuming that some additional photoabsorption takes place in the plume above the sample surface.[47] While this is expected, it is not always

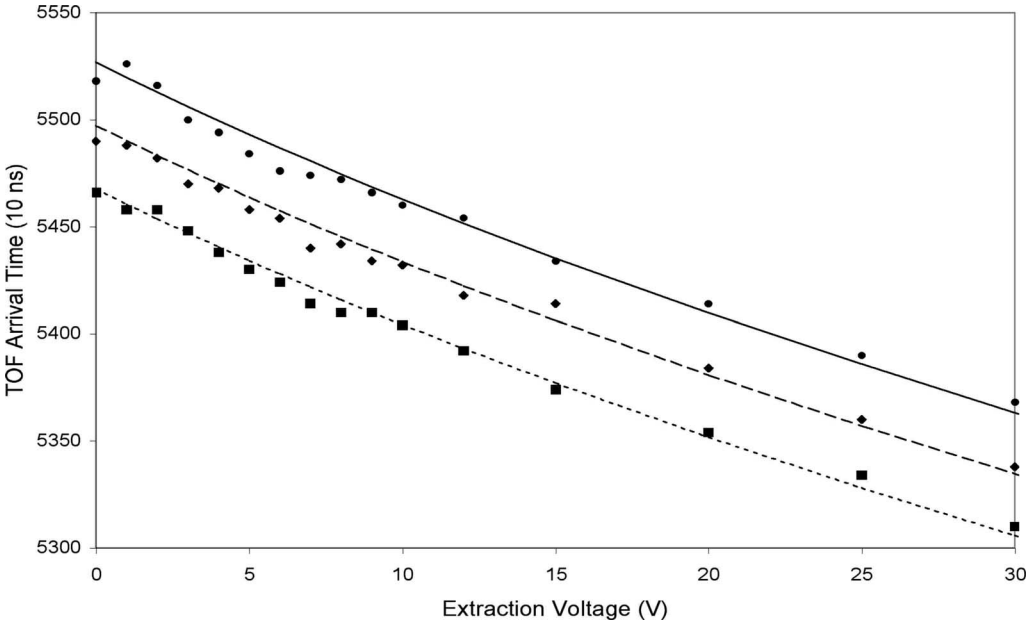

FIG. 5. Low extraction voltage detail of Fig. 4. Kinetic-energy determination of LID of tungsten. Experimental arrival times for peaks assigned to tungsten isotopes: 182 amu (squares); 184 amu (diamonds); and 186 amu (circles). Minor isotopes 180 and 183 amu are not indicated. The calculated ion arrival times with 22 eV initial kinetic energy are indicated as lines in the figure: 180 amu (solid line), 182 amu (dashed line), and 184 amu (dotted line). The overlap between ion isotope TOF peaks contributes to the mismatch between theoretical and experimental arrival times.

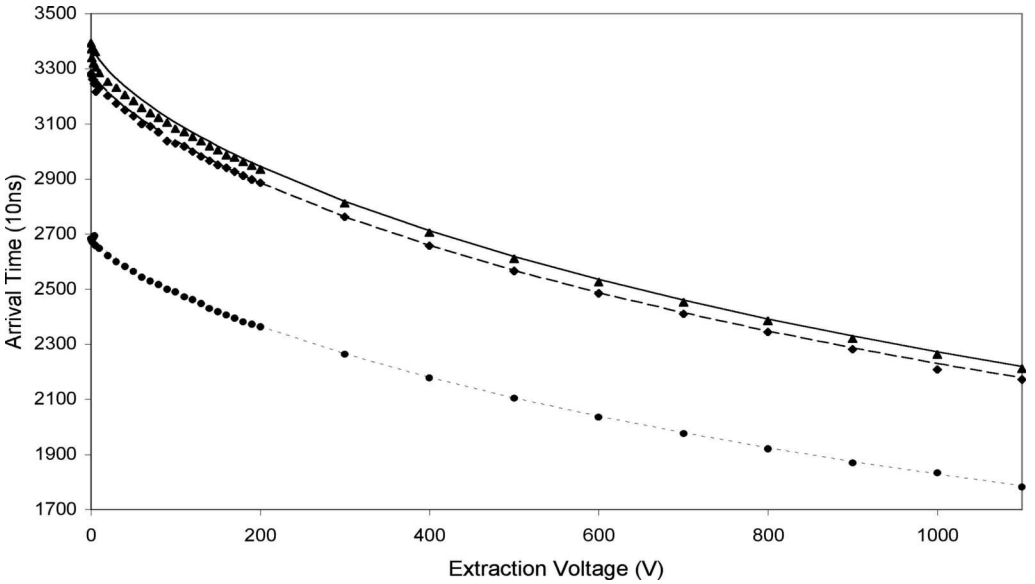

FIG. 6. Experimental arrival times for peaks assigned to nickel isotopes: 58 amu (diamonds) and 60 amu (triangles). Also shown are arrival time data for the 39 amu isotope of potassium (circles). The calculated ion arrival times include 30 eV of initial kinetic energy and are indicated (as a dashed line for 58 amu, a solid line for 60 amu, and a dotted line for 39 amu). The differences between the 60 amu isotope experimental data and calculated arrival times are attributed to a failure to completely resolve the nickel isotope peaks. The sample was held at 1200 V plus the indicated extraction voltage, and the voltage bias of the first plate of the mass spectrometer was measured to be 1200 V.

the case and stimulated desorption products in laser experiments have ranged from subthermal kinetic energies[32] to the high kinetic energies we report here. This range of results suggests that different physical processes are accessible under various experimental conditions.

In general, stimulated desorption mechanisms that can produce high-kinetic-energy ions, such as MGR, Knotek-Fiebelman, and Coulomb explosion model, lead to different ion kinetic energies for different ions from the same sample and in the case of Coulomb explosion the KE correlates with laser intensity. The fact that this is not the case in the present set of experiments points to a different physical picture. In this set of experiments, for a given surface, any ion that appears in the near-surface region is accelerated to the same kinetic energy.

Considering the relatively high ion kinetic energy and narrow distribution of ions that are peaked at the volume plasmon energy, it is very difficult to invoke a mechanism that explains our LID results and does not include the excitation of volume plasmons. Perhaps the best plausibility argument

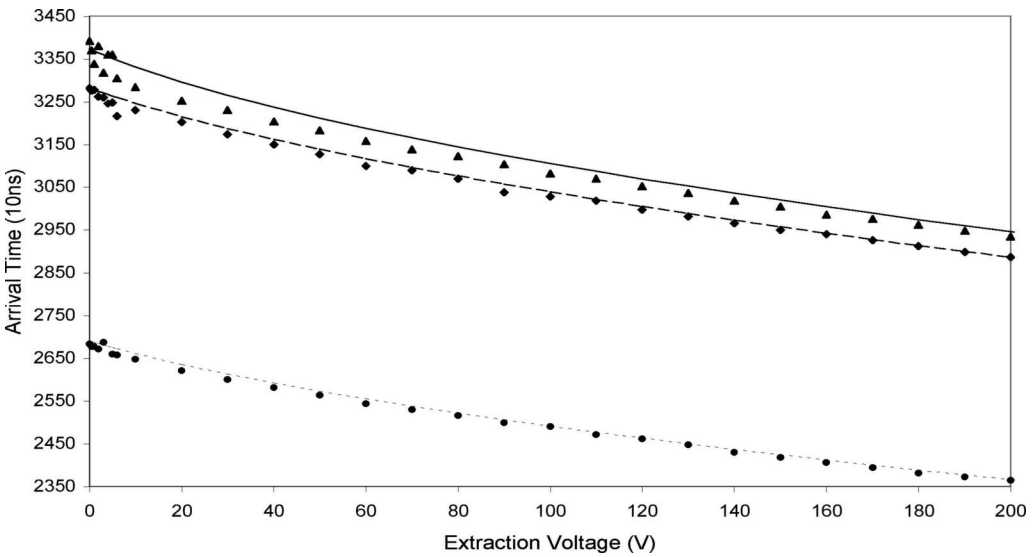

FIG. 7. Detail of Fig. 6. Experimental arrival times for peaks assigned to nickel isotopes: 58 amu (diamonds) and 60 amu (triangles). Also shown are arrival times data for the 39 amu isotope of potassium (circles). The isotope TOF arrival time peaks overlap, and this results in a shift of the unresolved peaks. The calculated ion arrival times include 30 eV of initial kinetic energy and are indicated (as a dashed line for 58 amu and as a solid line for 60 amu).

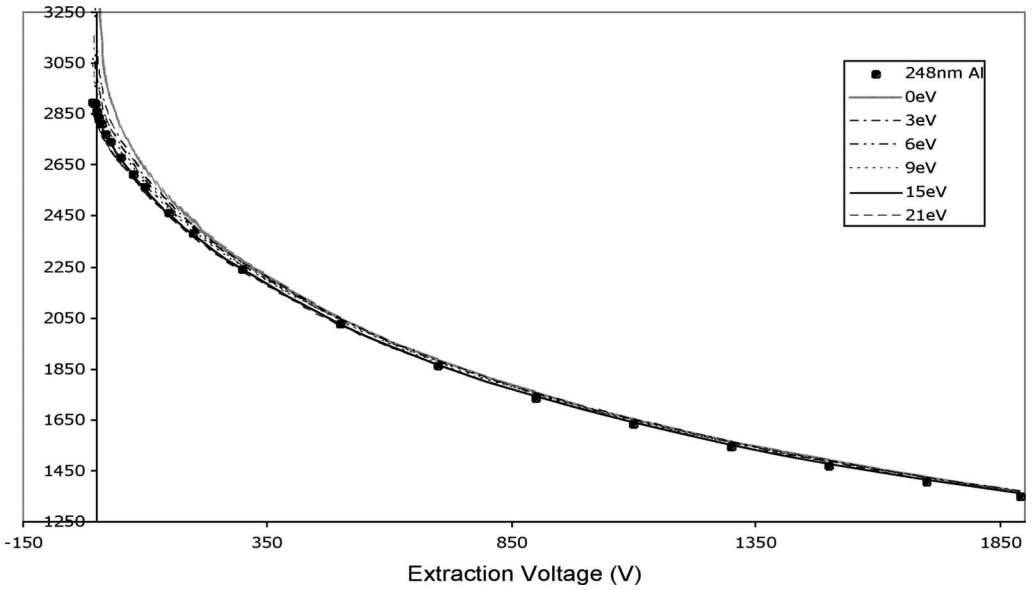

FIG. 8. Al^+ kinetic energy from TOF arrival time data and calculated arrival times for pulsed UV LID from Al(111). Calculated arrival times are presented, assuming several different initial ion kinetic energies (see legend).

supporting a volume plasmon excitation of an ion that can occur in this set of experiments is that it is known that the inverse process can occur in an ion exciting a volume plasmon.[48–50]

Our pulsed UV LID experiments appear to involve the transfer of momentum from a volume plasmon to a target metal ion in the near-surface region of a metal crystal. Such a process requires several things to happen. First, volume plasmons with energies of 15 eV or more must somehow be excited using a UV pulsed laser with photon energies of about 5 eV. Second, a rapid deexcitation process usually precludes the observation of target metal ions in stimulated desorption experiments such as electron stimulated desorption (ESD) or synchrotron Vacuum UltraViolet (VUV) PSD.[47] This near-surface relaxation process must not dominate the LID process or target metal ions would not be observed. Such a target metal near-surface ion or excited adatom must be screened from overlap with the band energy levels in the substrate. Third, a scattering event must occur in the near-surface region between an ion and a volume plasmon that culminates in the transfer of momentum to the departing ion. As pointed out in Ref. 38, the momentum transferred to the departing ion must come from the surface because the plasmon carries a small amount of momentum.

The interaction has to take place between volume plasmons and near-surface ions. This is possible because the vol-

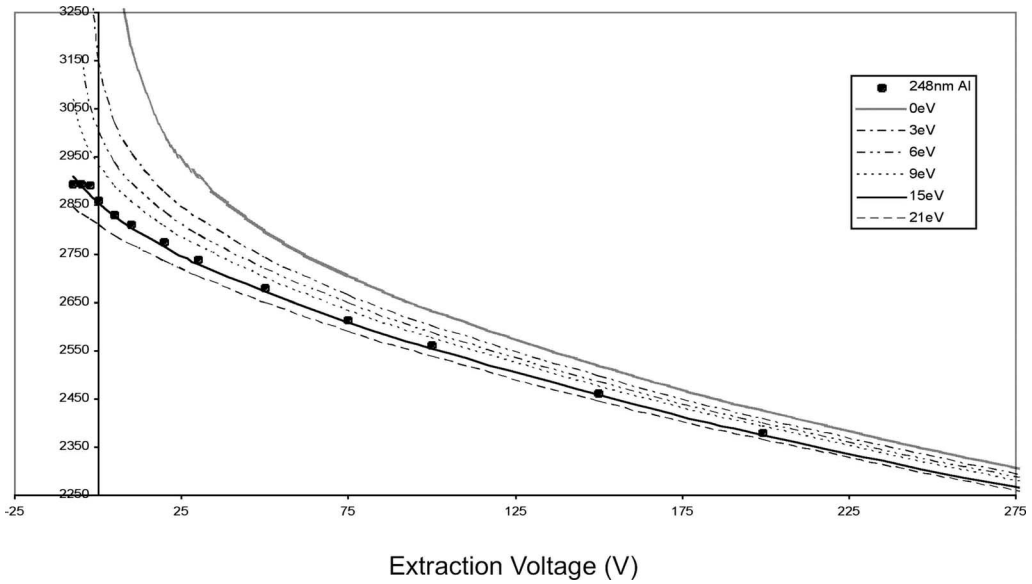

FIG. 9. Detail of Fig. 8: determination of Al^+ kinetic energy from TOF arrival time data and calculated arrival times for 248 nm pulsed LID from Al(111). The various lines indicate calculated arrival times assuming different initial kinetic energies and extraction voltages. The experimental arrival times are indicated as filled circles.

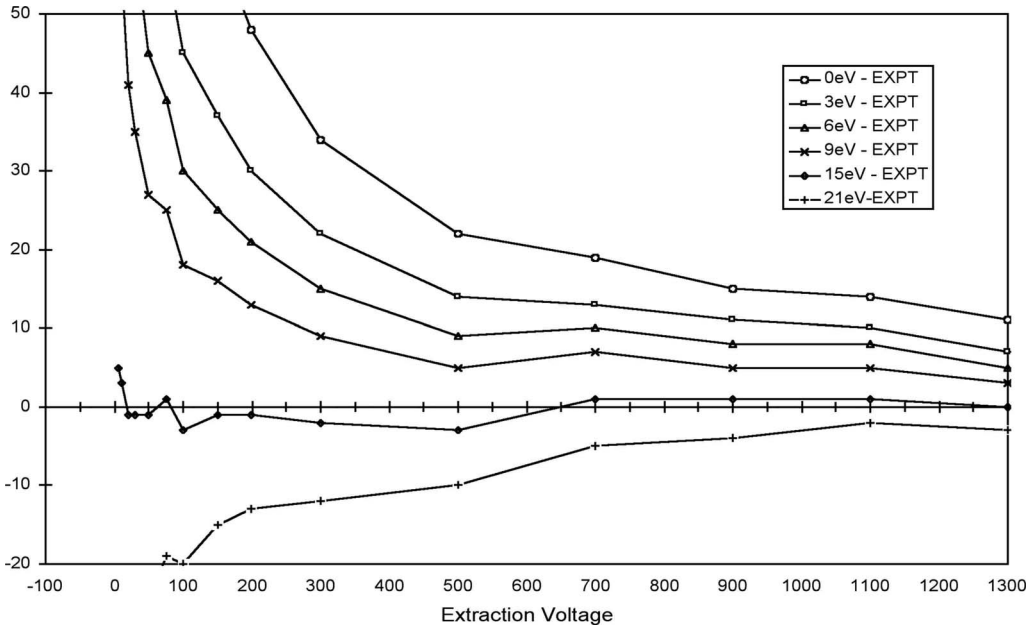

FIG. 10. The experimental arrival time is subtracted from the calculated arrival time in units of 10 ns. The sample was set to 700 V plus the indicated extraction voltage, and the voltage bias of the first plate of the mass spectrometer was measured to be 700 V.

ume plasmon extends slightly beyond the surface. Beraga *et al.*,[26] Barton,[51] Eguiluz,[52] and Nazarov and Luniakov[53] showed that electron-gas dispersion allows external probes to interact with volume plasmons.

How are volume plasmons excited in these pulsed UV LID experiments? Because the optical selection rules restrict the excitation of plasmons from a flat surface, the observation of surface plasmon excitation has been tied to arguments about real-world surface roughness. Some reports indicate that the amount of surface roughness required for this sort of excitation is much less rough than the surface of our metal crystals even after polishing.[54]

The most likely way to explain our results is that photoexcited surface plasmons excite volume plasmons. In this picture, a number of photons are required to excite a surface plasmon and it still takes more than one surface plasmon to excite a volume plasmon.

Surface plasmon excitation should be expected in a set of experiments such as this one. Surface plasmon excitation has been studied at least since the observation of Wood's anomaly.[55] Surface plasmon–enhanced multiphoton photoemission can also occur in this intensity regime.[56] Surface plasmon excitation has been observed using scanning near optical microscopy (see, for example, Ref. 57). It has been argued that in extraordinary optical transmission (EOT) experiments[58] the surface morphology on the front side of a metal film is sufficient to permit the photoexcitation of surface plasmons in a region around a small hole. In EOT experiments, surface plasmons can be excited on the walls of the hole and can radiatively decay on the back side of the metal film. In this set of LID experiments, photons impinging over an area in the vicinity of a surface defect in the metal surface can excite surface plasmons which can collectively lead to a high local electromagnetic field. In EOT experiments, there is typically a hole through the metal film that allows excitation of surface plasmons on the rear surface of the film and subsequent radiative decay. In our LID experiment, a surface defect in our thick metal crystal sample could lead to a similar surface plasmon excitation process to the one that occurs in the thin metal film during EOT experiments. However, detection of the radiative decay of a surface plasmon is observed on the back side of the thin metal film in the EOT experiment and this is not possible in the LID experiment. Instead surface plasmons can excite volume plasmons in the LID experiment. It is plausible that a high enough local electromagnetic field is present in the vicinity of the surface defect to excite volume plasmons. In this picture, the excitation of surface plasmons can be indirectly detected through the decay of the volume plasmons that contribute to the ion desorption process. It is plausible that a high enough local electromagnetic field is present in the vicinity of a surface defect to excite volume plasmons.

Another possibility is that the excitation of a surface plasmon as an intermediate step is not required. Both the photon skin depth in the metal and the volume plasmon extent outside of the surface into the vacuum are quite small, but they are not zero. A surface defect (or a set of defects perhaps including near-surface features) could permit photoabsorption and permit creation of a large-enough local electromagnetic field to excite a volume plasmon. A multiphoton absorption mechanism might be possible at these laser fluences with an accidental near-energy resonance and a rough real-world surface.[59]

Although a surface plasmon photoexcitation process seems more likely in this case, volume plasmon excitation is expected for ion penetration phenomena. While volume plasmon excitation might be a "minor process," it seems difficult to completely reject the inverse of this process out of hand. Consider a hot-electron picture.[60] If we view the laser interaction with the sample in terms of an inhomogeneous plasma

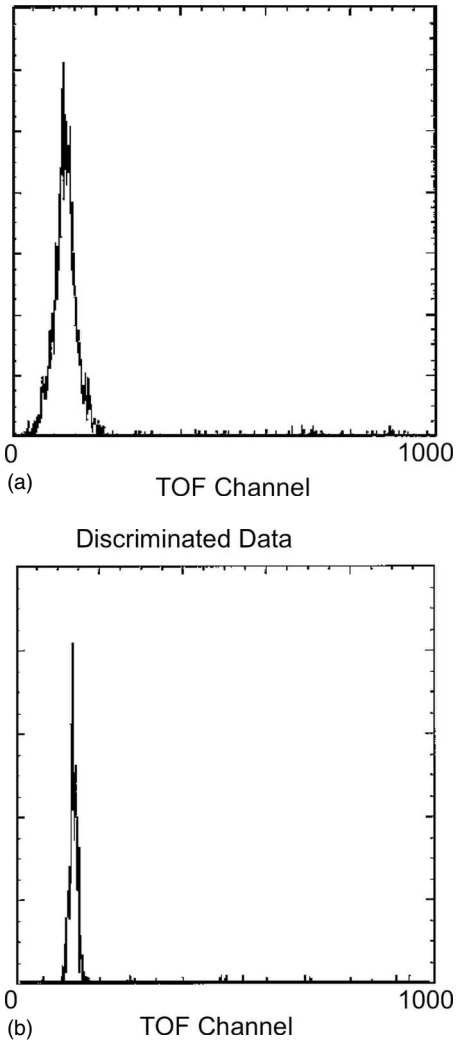

FIG. 11. (a) A sum of raw data (using only software threshold baseline suppression) of pulsed 248 nm LID TOF from Al(111) taken at 10 ns per channel for the time slice around the Al^+-ion arrival time. (b) A sum of software discriminated pulsed 248 nm LID TOF data from Al(111) taken at 10 ns per channel for the time slice around the Al^+-ion arrival time. The data set was created by summing only mass spectra from laser shots with single-ion Al^+ hits.

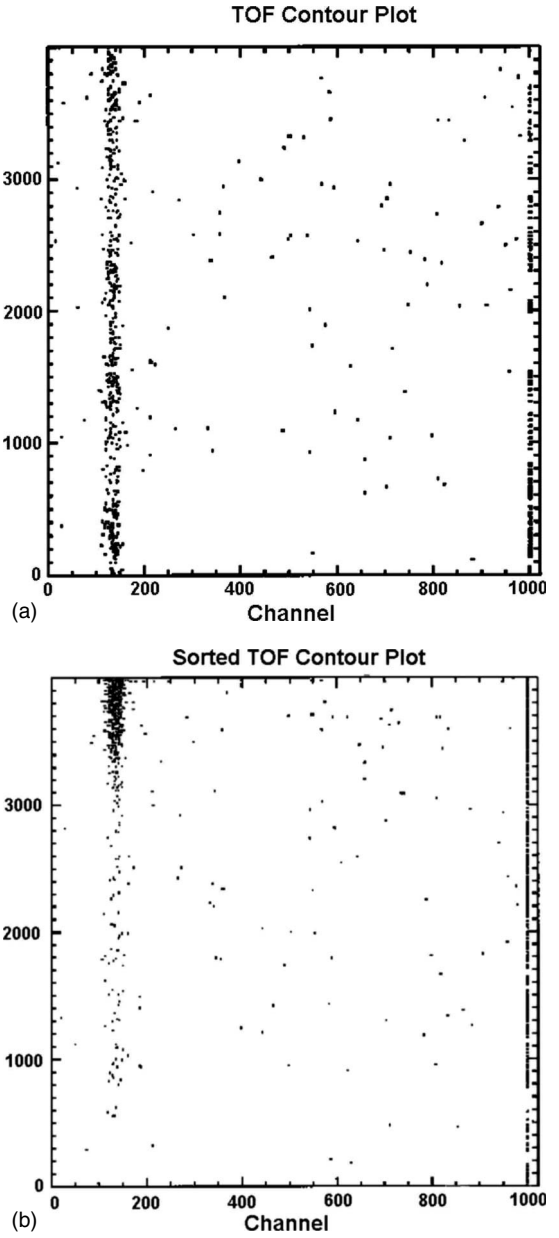

FIG. 12. Individual mass spectra from several thousand laser shots in a 248 nm LID TOF experiment on aluminum. (a) Raw data stack using only software threshold baseline suppression taken at 10 ns per channel for the time slice around the Al^+-ion arrival time. (b) The same mass spectra data set arranged vertically to discriminate spectra with multiple aluminum-ion hits. By including only mass spectra with single aluminum ions in the sum, the software discrimination is used to suppress the space-charge effects on the distribution of ion energies.

because of the nonideal surface boundary, the small skin depth of the metal, the material imperfections, and the interaction of these factors with variations in the laser beam, it should still be possible to excite a volume plasmon by producing a hot electron.

Another reason not to be quick to reject a volume plasmon excitation mechanism that does not require surface plasmon excitation is that we do not observe a surface plasmon kinetic-energy signature in the ions measured in this set of LID experiments. While one might have expected surface plasmon excitation to be accompanied by the excitation of a combination of multimode plasmons and volume plasmons, this was not observed. This set of LID experiments observed only ions with the volume plasmon kinetic energy. Perhaps this observation is a consequence of the geometry of our experimental setup; since only ions ejected within a small solid angle around the surface normal are detected, the angle may select ions with a kinetic-energy kick from volume plasmon excitations which are perpendicular to the surface.

Note that plasmon excitation processes might also provide a way to pool energy. Extraordinary optical transmission provides a model of how this can work through the excitation of surface plasmons by collecting photons that impinge on an area of the surface around a defect. This argues for a surface plasmon excitation to collect the energy from a number of

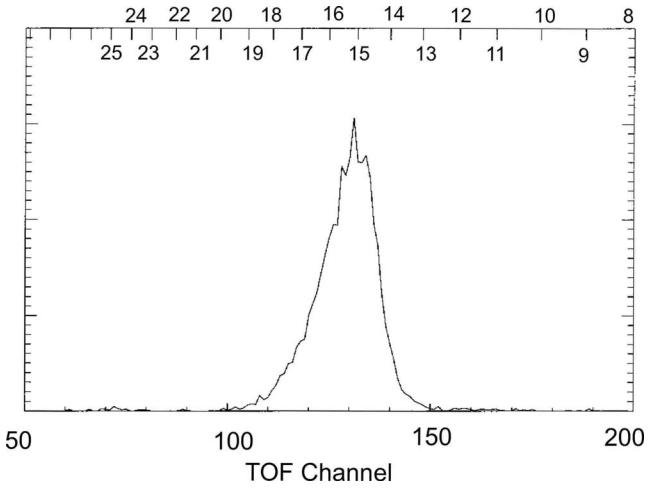

FIG. 13. Another presentation of the software discriminated ion peak for aluminum from this pulsed 248 nm LID TOF experiment. Arrival time in addition to a contant offset is indicated on the bottom axis and aluminum-ion kinetic energy (eV) for mass 27 is indicated on the top axis of the figure. Full width at half maximum for the aluminum TOF peak is approximately 2 eV.

photons. But volume plasmons are also delocalized excitations and could also provide a way to pool energy. In either case, this could address a long-standing problem: stimulated desorption experiments often require a way to pool energy from many photons and collect it on the desorbing species.

The possibility of a delocalized excitation that can decay locally at a lattice defect, impurity site, adatom, surface, or surface irregularity changes the usual physical picture for this sort of process. Instead of requiring a number of photons to collect locally at an adatom during a brief time before deexcitation can occur, a plasmon excitation can take place by several photons impinging over an area of the sample surface. Ion excitation can occur locally by the decay of a volume plasmon at the defect. The excited ion can also be screened by a volume plasmon, thus reducing the importance of the near surface ion–bulk interaction in the ion deexcitation process. The volume plasmon also provides a kinetic energy kick to ion desorption through the plasmon–ion–surface interaction described by Ritchie, Manson, and Echenique for surface plasmons in Ref. 38.

This sort of physical picture involving volume plasmon interaction is at least somewhat compatible with the physical picture that is accepted by the stimulated desorption community. The desorption mechanism of the Itoh multiple-hole localization conjecture could be facilitated by such a plasmon decay at an adatom or another desorption site.[61,62] The Itoh picture[63] was developed to explain stimulated desorption in semiconductors, but it has been applied more generally. The associated idea of a population of electrons and holes arising from a plasmon decay fits in well with parts of this type of physical picture.

TABLE I. Comparison of our measured results with both theoretically predicted and experimental volume plasmon energies listed in the book by Pines (Ref. 46).

Element	Ion KE (this work) (eV)	Theoretical plasmon energy (eV)	Experimental plasmon energy (eV)
Al	15 ± 2	16	15
W	22 ± 3	23	22
Ni	30 ± 5	35	23

The laser intensity dependence of the Al^+-ion yield in this LID experiment was measured to be roughly $I^{7\pm2}$. The other LID samples seem to exhibit an even higher-order ion desorption yield dependence on laser intensity. In a rate equation picture, these data would indicate that we are looking at a process that requires about seven photons. Often these high-order yield dependencies in laser stimulated desorption experiments are regarded as indicating a thermal threshold or an excited-state-density threshold associated with the desorption process. The usual threshold picture also does not seem to offer a particular insight as to why we should measure $I^{7\pm2}$ instead of some other order in the yield of our pulsed 248 nm LID experiment on aluminum. The preceding description of a stimulated desorption experiment changes considerably with inclusion of a volume plasmon excitation. In the case of aluminum, if two 15 eV volume plasmons are excited, requiring about six 5 eV photons as the rate limiting step, then this fundamental electronic excitation in the material might provide an accessible near resonance. The first multiple of the volume plasmon resonance energy with sufficient total energy to lead to ion desorption could help explain why a specific high-order laser fluence dependence on stimulated desorption ion yield has been observed in some experiments.

Control of laser polarization should allow us to distinguish between several of the different possible processes. It was hoped that by measuring the laser power for every laser shot, storing every associated TOF mass spectrum, and varying the laser polarization it would be possible to pursue this issue experimentally. Instead, what was observed was that the "active" and "quiet" periods associated with stimulated desorption ion yield bursting dominated any changes associated with laser polarization. Even the laser power measurements were performed by averaging over active and quiet bursting periods of desorption yield. The active and quiet bursting periods have been tentatively associated with laser induced changes to the surface. It might be noted that some EOT experiments that involve decorating the metal film surface around the through hole have observed changes in the patterning around the hole.

V. CONCLUSION

Pulsed UV LID experiments at 248 nm have been performed on several single-crystal metal samples: Al(111), W(100), and Ni(111). It has been found that for each sample the kinetic-energy distribution of the desorbed ions is sharply peaked at the volume plasmon energy. This follows some earlier LID experiments starting with Ag(111).[33] The Al(111) experiment has been refined here at 248 nm, and tungsten and nickel samples have also been studied.

The experimental results for pulsed UV LID experiments conducted below laser fluences associated with surface melt-

ing on several metal single-crystal samples under UHV conditions have converged on ion kinetic energies that are sharply peaked at the volume plasmon energy. These results can be understood with the surface plasmon annihilation model of Ritchie *et al.*[38] modified to allow volume plasmon annihilation model. This approach was suggested by Ritchie *et al.*[39]

The acceleration of an ion through interaction with an electromagnetic wave at the surface of a conductor provides relatively unambiguous evidence that volume plasmons are excited in the single-crystal metal samples during these LID experiments. Our data indicate that the pulsed UV laser photons can excite volume plasmons in the metal sample with quantum energies three or more times the energy of a single photon. This experimental observation provides strong support for the notion that volume plasmons can play an important role in laser-surface interactions.

We point out that volume plasmon excitation can explain other aspects of this set of pulsed UV LID experiments as well as some related work. First, the volume plasmon can screen the near-surface excitation. Second, the nonlocal volume plasmon provides a way to pool the energy from a number of photons and deposit it locally near a stimulated desorption site. Third, volume plasmon decay provides a way to deposit energy at the surface and in the near-surface region in the vicinity of a defect. It might also account for changes in surface morphology. Plasmon decay at defect sites and surface irregularities can help explain desorption yield bursting, and the associated aggregation of defects would help explain a depression of the laser ablation threshold over laser exposure. The decay of volume plasmons into surface plasmons and surface acoustic waves could also help to produce the surface modification observed in some laser experiments.

ACKNOWLEDGMENTS

This work was funded by USAFOSR under Contract No. F04701-93-C-0094. The support of program manager Howard Schlossberg of AFRL/USAFOSR/NE is gratefully acknowledged. Additional funding was provided by The Aerospace Corporation as part of an internal research and development program. We appreciate and acknowledge helpful discussions with R. Ritchie, R. Manson, P. Echinque, J. Reif, T. Orlando, and M. Sieger. We also wish to thank Phillip M. Johnson and William W. Hansen for valuable help with hardware and software.

*david.p.taylor@aero.org

[1] D. Claesson, S.-A. Lindgren, L. Walldén, and T.-C. Chiang, Phys. Rev. Lett. **82**, 1740 (1999).
[2] P. Martin, R. Trainham, P. Agostini, and G. Petite, Phys. Rev. B **45**, 69 (1992).
[3] M. L. Knotek and P. J. Feibelman, Phys. Rev. Lett. **40**, 964 (1978).
[4] P. A. Redhead, Can. J. Phys. **42**, 886 (1964).
[5] D. Menzel and R. Gomer, J. Chem. Phys. **40**, 1164 (1964).
[6] G. Ferrini, A. Viggiani, D. Sertore, P. Michelato, and F. Parmigiani, Phys. Rev. B **60**, 8383 (1999).
[7] J. H. Bechtel, W. Lee Smith, and N. Bloembergen, Phys. Rev. B **15**, 4557 (1977).
[8] H. Yamakoshi, C. T. Chin, S. Jaimungal, P. R. Herman, L. Zhao, G. Kulcsar, F. W. Budnik, and R. S. Marjoribanks, Rev. Sci. Instrum. **65**, 1964 (1994).
[9] M. Fleischmann, P. J. Hendra, and A. J. McQuillan, Chem. Phys. Lett. **26**, 163 (1974).
[10] T.-K. Lee and J. L. Birman, Phys. Rev. B **22**, 5961 (1980).
[11] M. Aeschlimann, C. A. Schmuttenmaer, H. E. Elsayed-Ali, R. J. D. Miller, J. Cao, Y. Gao, and D. A. Mantell, J. Chem. Phys. **102**, 8606 (1995).
[12] P. Martin, S. Guizard, and G. Petite, J. Appl. Phys. **76**, 2264 (1994).
[13] T. Vartanyan, M. Simon, and F. Träger, Appl. Phys. B: Lasers Opt. **68**, 425 (1999).
[14] S. Link, Z. L. Wang, and M. A. El-Sayed, J. Phys. Chem. B **103**, 3529 (1999).
[15] R. L. Hettich, R. N. Compton, and R. H. Ritchie, Phys. Rev. Lett. **67**, 1242 (1991).
[16] D. Ding, J. Huang, R. N. Compton, C. E. Klots, and R. E. Haufler, Phys. Rev. Lett. **73**, 1084 (1994).
[17] S. Hunsche, T. Starczewski, A. l'Huillier, A. Persson, C. G. Wahlstrom, H. B. van Linden van den Heuvell, and S. Svanberg, Phys. Rev. Lett. **77**, 1966 (1996).
[18] H. Chen, J. Boneberg, and P. Leiderer, Phys. Rev. B **47**, 9956 (1993).
[19] H. Helvajian, Proc. SPIE **2403**, 2 (1995).
[20] R. A. Baragiola, C. A. Dukes, and P. Riccardi, Nucl. Instrum. Methods Phys. Res. B **182**, 73 (2001).
[21] S. J. Smith and E. M. Purcell, Phys. Rev. **92**, 1069 (1953).
[22] J. P. Bachheimer, Phys. Rev. B **6**, 2985 (1972).
[23] Y.-M. Shin, J.-K. So, K.-H. Jang, J.-H. Won, A. Srivastava, and G.-S. Park, Phys. Rev. Lett. **99**, 147402 (2007).
[24] N. E. Glass, Phys. Rev. A **36**, 5235 (1987).
[25] J. B. Pendry and L. M. Moreno, Phys. Rev. B **50**, 5062 (1994).
[26] A. Bergara, J. M. Pitarke, and R. H. Ritchie, Phys. Lett. A **256**, 405 (1999).
[27] D. P. Taylor, W. C. Simpson, K. Knutsen, M. A. Henderson, and T. M. Orlando, Appl. Surf. Sci. **101**, 127 (1998).
[28] T. Götz, M. Bergt, W. Hoheisel, F. Träger, and M. Stuke, Appl. Phys. A: Mater. Sci. Process. **63**, 315 (1996).
[29] G. Petite, P. Martin, R. Trainham, P. Agostini, S. Guizard, F. Jollet, J. P. Durand, K. Bohmer, and J. Rief, *Laser Ablation: Mechanisms and Applications*, Lecture Notes in Physics Vol. 389 (Springer-Verlag, Berlin, 1991), p. 127.
[30] R. F. Haglund and R. Kelly, *Sputtering of Atoms and Molecules (SPUT92): Electronic Processes in Sputtering by Laser Beams in Fundamental Processes* (Royal Danish Academy of Sciences and Letters, Copenhagen, 1993), p. 527.
[31] T. D. Bennett, D. J. Krajnovich, and C. P. Grigoropoulos, Phys. Rev. Lett. **76**, 1659 (1996).

[32] K. M. Beck, D. P. Taylor, and W. P. Hess, Phys. Rev. B **55**, 13253 (1997).
[33] W. Hoheisel, M. Vollmer, and F. Träger, Phys. Rev. B **48**, 17463 (1993).
[34] H. Helvajian and R. Welle, J. Chem. Phys. **91**, 2616 (1989).
[35] M. J. Shea and R. N. Compton, Phys. Rev. B **47**, 9967 (1993).
[36] H. S. Kim and H. Helvajian, J. Phys. Chem. **95**, 6623 (1991).
[37] D. P. Taylor and H. Helvajian, Surf. Sci. **451**, 68 (2000).
[38] R. H. Ritchie, J. R. Manson, and P. M. Echenique, Phys. Rev. B **49**, 2963 (1994).
[39] Rufus H. Ritchie *et al.* (private communication).
[40] D. P. Taylor and H. Helvajian, Proc. SPIE **3618**, 170 (1999).
[41] M. Wu, D. P. Taylor, and P. M. Johnson, J. Chem. Phys. **94**, 7596 (1991).
[42] M. Wu, D. P. Taylor, and P. M. Johnson, J. Chem. Phys. **95**, 761 (1991).
[43] D. P. Taylor and P. M. Johnson, J. Chem. Phys. **98**, 1810 (1993).
[44] D. P. Taylor, J. G. Goode, J. E. LeClaire, and P. M. Johnson, J. Chem. Phys. **103**, 6293 (1995).
[45] H. Raether, *Surface Plasmons*, Springer Tracts in Modern Physics Vol. 111 (Springer, Berlin, 1988).
[46] D. Pines, *Elementary Excitations in Solids* (Addison-Wesley, New York, 1963).
[47] W. C. Simpson, K. Knutsen, M. A. Henderson, and T. M. Orlando, *Proceedings of COLA '97* (North-Holland/Elsevier, New York, 1988), p. 101.
[48] W. Drube and F. J. Himpsel, Phys. Rev. Lett. **60**, 140 (1988).
[49] D. P. Woodruff and N. V. Smith, Phys. Rev. B **41**, 8150 (1990).
[50] R. A. Baragiola and C. A. Dukes, Phys. Rev. Lett. **76**, 2547 (1996).
[51] G. Barton, Rep. Prog. Phys. **42**, 963 (1979).
[52] A. G. Eguiluz, Solid State Commun. **21**, 33 (1981).
[53] V. U. Nazarov and Y. V. Luniakov, Phys. Rev. B **52**, 12414 (1995).
[54] F. J. Garcia-Vidal and J. B. Pendry, Phys. Rev. Lett. **77**, 1163 (1996).
[55] R. W. Wood, Phys. Rev. **48**, 928 (1935).
[56] T. Tsang, T. Srinivasan-Rao, and J. Fischer, Phys. Rev. B **43**, 8870 (1991).
[57] S. I. Bozhevolnyi, V. S. Volkov, E. Devaux, J.-Y. Laluet, and T. W. Ebbesenr, Nature (London) **440**, 508 (2006).
[58] T. W. Ebbesen, H. J. Lezec, H. F. Ghaemi, T. Thio, and P. A. Wolf, Nature (London) **391**, 667 (1998).
[59] E. C. Le Ru, P. G. Etchegoin, and M. Meyer, J. Chem. Phys. **125**, 204701 (2006).
[60] J. W. Gadzuk, *Desorption Induced by Electronic Transitions IV* (Springer, Berlin, 1990), p. 85.
[61] N. Itoh and T. Nakayama, Phys. Lett. **89A**, 211 (1982).
[62] H. Sumi, Surf. Sci. **248**, 382 (1991).
[63] N. Itoh, K. Hattori, Y. Nakai, J. Kanasaki, A. Okano, and J. Richard F. Haglund, *Laser Ablation: Mechanisms and Applications*, Lecture Notes in Physics Vol. 389 (Springer-Verlag, Berlin, 1991), pp. 213–223.